Theoretical Characterization of Intramolecular Proton Transfer in the Ground and the Lowest-Lying Triplet Excited States of 1-Amino-3-Propenal: A Methodological Comparison

MARTA FORÉS,[1] MIQUEL DURAN,[1] MIQUEL SOLÀ,[1] LUDWIK ADAMOWICZ[2]

[1]*Institut de Química Computacional and Departament de Química, Universitat de Girona, 17071 Girona, Catalonia, Spain*
[2]*Department of Chemistry, University of Arizona, Tucson, Arizona 85721*

Received 29 July 1999; accepted 18 October 1999

ABSTRACT: Several theoretical methods are employed to characterize the intramolecular proton transfer in the ground state and in the lowest-lying $^3n\pi^*$ and $^3\pi\pi^*$ excited states of 1-amino-3-propenal. The geometrical parameters, the relative energy of the two tautomeric forms, the energy barrier for the proton transfer, and the energy difference between the ground and the excited states predicted by the different methods are compared. It was found that: (1) the CASPT2 results are in good agreement with those obtained using the CCSD(T) method; (2) the CIS method and the CASSCF method with a medium-sized active space yield poor geometries and overestimate the adiabatic energy excitations and the energy barriers for the proton transfer; and (3) the B3LYP method provides good adiabatic excitation energies, although B3LYP energy barriers are

Correspondence to: M. Solà; e-mail: miquel@iqc.udg.es
Contract/grant sponsor: Spanish DGICYT; contract/grant numbers: PB95-0762 and PB98-0457-C02-02
Contract/grant sponsor: European Union; contract/grant number: CI1*-CT93-0339
Contract/grant sponsor: Generalitat de Catalunya; contract/grant number: CIRIT FI/96-05011.1
This article includes Supplementary Material available from the authors upon request or via the Internet at ftp.wiley.com/public/journals/jcc/suppmat/21/257 or http://journals.wiley.com/jcc/

© 2000 John Wiley & Sons, Inc.

systematically underestimated. For qualitative studies of ESIPT processes in more extended molecular systems, in which computational cost prevents the use of advanced post-Hartree–Fock methods, the CIS-MP2//CIS methodology is recommended. However, we have not found a low-cost method among the methods studied that is capable of providing a quantitative description of the proton-transfer processes. If such a description is required, we recommend the use of single-point CASPT2 calculations with a medium-sized active space performed using CIS-optimized geometries. © 2000 John Wiley & Sons, Inc.
J Comput Chem 21: 257–269, 2000

Keywords: Excited-state intramolecular proton transfer (ESIPT); hydrogen bond; coupled-cluster method (CC); B3LYP; CIS; CIS-MP2; CASSCF; CASPT2; methodological comparison; 1-amino-3-propenal

Introduction

Excited-state intramolecular proton transfer (ESIPT) has received a great deal of attention, both from experimental and theoretical points of view, due to its potential application in several fields. Laser activity,[1,2] data storage and optical switching devices,[2,3] Raman filters, and hard-scintillation counters[4] are some of the possible practical uses of compounds in which ESIPT processes occur. Moreover, the useful photochemistry of many polymer photostabilizers has been attributed in part to ESIPT reactions.[5–7] Finally, in the biological field, ESIPT processes have been suggested as possible mechanisms involved in spontaneous genetic mutations.[8,9]

In ESIPT processes, the absorption of a photon causes a proton to be transferred within a molecule between donor and acceptor groups. These photoinduced reactions usually happen very fast,[10] and can be attributed to the barrierless character of such processes. A number of *ab initio* calculations have been done to study the ESIPT in small systems.[11–26] However, it has been proven that small systems are not always good models for the larger molecules most frequently considered in the experimental studies, and that larger models are required to obtain results relevant to the experimental works.[26–28] On the other hand, it has been well established that an accurate evaluation of the energy parameters governing the proton transfer requires use of extended basis sets and inclusion of correlation effects.[29–34] However, the use of sophisticated methods to study larger molecular systems is often impractical due to the very demanding nature of computations involved in such studies. Thus, for theoretical investigations of ESIPT in such molecules it is of critical importance to find adequate yet simple molecular models, and to choose a computational method capable of describing, at least qualitatively, the structural and energetic parameters of the ESIPT processes.

The unrestricted Hartree–Fock method (UHF) can be applied to study the lowest-lying excited states of a given symmetry and/or multiplicity. However, because, in general, the UHF wave function is not an eigenfunction of the S^2 operator, it can include some contributions from states with other multiplicities than the multiplicity of the considered state (spin contamination). The advantage of the UHF method, however, is that it can be applied to large molecular systems. Another approach that is computationally simple enough to use in electron excitation calculations of large systems is the configuration interaction method with single excitations (CIS).[35,36] The spin-contamination problem does not occur in this method if the reference wave function is a spin-restricted determinant (open or closed shell). However, the CIS method has been known to often produce large errors in excitation energies and is also unable to describe states that have a significant double-excitation character.[37,38] Furthermore, in the calculations of ESIPT processes, often the CIS methodology has given overly high energy barriers.[15,16,18,24,26,33,39] Therefore, a method that describes correlation effects better than CIS, yet is still able to handle ESIPT in larger molecular systems, is needed.

There are several methods to account for the electron correlation effects in electronic excited states. This can be done via second-order Møller–Plesset perturbation theory in combination with the unrestricted Hartree–Fock (UMP2) wave function or the CIS (CIS-MP2) wave function.[36] It should be noted, however, that the spin contamination of the UHF wave function is not significantly reduced by low-order perturbation corrections.[40] On the other hand,

in methods where through iterations the correlation corrections are accounted for to a higher order—like in the unrestricted coupled-cluster (UCC)[41–47] or unrestricted quadratic configuration interaction (UQCI)[48] methods based on the UHF wave function — the spin contamination is less severe.[40, 49–51] The states involving a simultaneous promotion of two or more electrons from the ground-state configuration are not always well described by these theories. An alternative approach is the complete active space multiconfiguration self-consistent-field (CASSCF) method, which employs the wave function in the form of a complete configuration expansion generated with a given set of active orbitals.[52] A limited description of the dynamic electron correlation effects by CASSCF with small active spaces can be corrected perturbatively by employing the CASPT2 method,[53–55] which is based on the second-order perturbation theory applied to the CASSCF wave function.

Unfortunately, the more refined the method becomes, the higher the computational effort required to perform calculations, thus excluding the most sophisticated *ab initio* approaches from their use in calculations of large molecular systems. An alternative to the conventional *ab initio* post-Hartree–Fock methods has often been found using density functional theory (DFT).[56–59] Although some formal and practical difficulties may result from the absence of an explicit multideterminantal wave function in treating open-shell systems by this approach,[59, 60] the potential utility of DFT in dealing with much larger systems than can be handled by state-of-the-art, correlated *ab initio* methods is an important advantage of this method. The question that has not been explored adequately is whether DFT can provide a correct description of ESIPT processes in the lowest-lying states of a particular symmetry and multiplicity.

In the present work, the proton transfer of 1-amino-3-propenal in the ground state and two lowest-lying triplet excited states is analyzed at different levels of theory. Study of the triplet excited states is relevant because they play an important role in fluorescence[61] and in the photochemistry of hydrogen-bonded DNA bases.[62] The aim of this work is to assess which levels of theory can describe ESIPTs in 1-amino-3-propenal with sufficient accuracy, yet at a reasonable computational cost that can be recommended for use in larger molecular systems. 1-Amino-3-propenal was proposed as a model of a group of systems studied experimentally that have the common NCCCO skeleton,[12] such as 2-(2′-hydroxyphenyl)oxazole,[18] 2-(2′-hydroxyphenyl)benzimidazole,[63] and 2-(2′-hydroxyphenyl)benzoxazole.[64, 65] Given that larger molecular models are required to study ESIPT in the aforementioned systems,[27, 28] methods cheaper than conventional *ab initio* correlated techniques, yet accurate enough to provide a reliable description of the process, are required.

Computational Details

In the first step, structural optimizations of the enol and keto tautomers of 1-amino-3-propenal and the transition state (TS) connecting the two structures were performed using the HF method for the ground state and the CIS method for the two lowest-lying triplet excited states, $^3n\pi^*$ and $^3\pi\pi^*$. Next, the same structural optimizations were also performed using the QCISD method[48] and the DFT method with the B3LYP functional,[56–59] which includes Becke's three-parameter nonlocal correction for exchange[66] and the Lee–Yang–Parr nonlocal correction for correlation.[67] Different investigators have shown that the B3LYP functional is the best currently available DFT functional to describe proton-transfer reactions.[25, 68–71] The structures obtained from the optimizations were tested by performing frequency calculations. These tests showed that each located transition state has an imaginary frequency corresponding to the transition mode describing the motion of atoms during the proton-transfer process.[72]

Among the aforementioned optimized structures we consider the QCISD results to be the most reliable, and they will be used as a reference to evaluate the accuracy of the results obtained with the other methods. To generate the reference energy values at the equilibrium and transition points, we performed CCSD(T)[46] calculations at the QCISD-optimized geometries. These results will be referred to as CCSD(T)//QCISD. The CCSD(T) method is a highly accurate approach in which the contributions from the single and double excitations are determined using an iterative procedure, thus accounting for the corresponding correlation effects to a high order, and the contributions from the triple excitations are accounted for using a noniterative approach and the converged configuration amplitudes of the single and double excitations.[73, 74] In calculations of the triplet excited states using DFT, QCISD, and CCSD(T) methods, the unrestricted formalism was used. At the B3LYP level, the S^2 values for the enol, keto, and the TS forms were 2.009, 2.011, and 2.007, respectively, for the $^3\pi\pi^*$ state, and 2.027,

2.025, and 2.030, respectively, for the $^3n\pi^*$ state. These values show that the UB3LYP wave function remains essentially spin pure along the whole range of the reaction coordinate. In general, spin contamination in UDFT is less severe than in UHF.[25, 75–78] Also, based on previous results,[50] we would expect almost no spin contamination in the UQCISD and UCCSD(T) wave functions.

Next, we performed single-point energy calculations for the ground and the two excited states at the MP2//HF and CIS-MP2//CIS[36] levels of theory. The frozen core approximation was used in the MP2 and CIS-MP2 calculations, whereas excitations from all orbitals were included in the CIS calculations. We also included CASSCF[52] calculations in the methodological comparison. CASSCF geometry optimizations for the keto, enol, and TS forms were performed. CASSCF single-point energy calculations were also done at the CIS-, B3LYP-, and QCISD-optimized geometries (CASSCF//CIS, CASSCF//B3LYP, CASSCF//QCISD). In all these calculations the (2, 5; 8) active space was used, where the first two numbers indicate the number of orbitals of a' and a'' symmetry included in the active space, respectively, and the third number refers to the number of active electrons. This medium-sized active space was found to yield a description of the ESIPT processes similar to that provided by larger active spaces in 1-amino-3-propenal[79] and in malonaldehyde.[80] Finally, CASPT2[53–55] single-point energy calculations were carried out for all optimal geometries found in the CIS, B3LYP, QCISD, and CASSCF calculations (CASPT2//CIS, CASPT2//B3LYP, CASPT2//QCISD, CASPT2//CASSCF). The results of the calculations were used in the analyses of the performance of the methods, which are described in the next section.

The double-zeta gaussian basis set of Dunning and Hay with polarization functions (D95**)[81] has been used throughout. In some B3LYP calculations, the D95** basis set was augmented with diffuse functions.[82] A deeper and systematic analysis of the effect of the basis set has not been pursued in this work. It should be noted that previous results on the barrier of the intramolecular proton transfer in the ground state of malonaldehyde[25] indicate that, starting from a double-zeta plus polarization basis set, a further extension of the basis set at the HF, MP2, and B3LYP levels of theory does not introduce significant modifications.

CASSCF and CASPT2 results were obtained by using MOLCAS-3[83] and -4[84] programs, whereas the remaining calculations were done using the GAUSSIAN-94[85] program.

Results and Discussion

GEOMETRICAL PARAMETERS

Table I summarizes the most relevant geometrical parameters for the ground state of 1-amino-3-propenal computed using the HF, DFT, QCISD, and CASSCF methods. In principle, CASSCF and QCISD should provide more reliable geometries than DFT and HF. CASSCF and QCISD yielded similar bond distances for the NCCCO backbone, but larger differences were found between these methods and DFT, with the DFT NCCCO bond lengths being closer to the QCISD results than to the CASSCF results. It is usually the case that, when a method overestimates the correlation effects, the double- and single-bond distances become more similar.[25] This is the trend that we observed in the B3LYP results upon comparison with the QCISD and CASSCF results. For instance, although the difference between the length of the N_1—C_2 (double) and the C_2—C_3 (single) bonds for the enol form (see Fig. 1) was 0.159 and 0.164 Å at the QCISD and CASSCF levels, respectively, it was only 0.139 Å at the DFT level. Thus, the tautomeric structures were overconjugated at the DFT level and this method seems to exhibit similar symptoms in geometry optimizations as the methods that overestimate the correlation effects. As expected, both the single- and double-bond lengths predicted by HF were smaller than the corresponding QCISD and CASSCF bond lengths.

For the structural parameters involved in the intramolecular hydrogen bond, CASSCF and QCISD provided values that were considerably different. For instance, the N_1—O_5 bond distance for the enol and keto forms was larger by 0.129 and 0.111 Å, respectively, at the CASSCF than at the QCISD level. Also, the N_1—H_6 bond distance in the enol form and the H_6—O_5 bond distance in the keto form were larger at the CASSCF level, indicating that the CASSCF enol and keto structures are more distant from the TS point for the proton transfer reaction than the QCISD structures. Surprisingly, the tautomeric HF structures were closer to the TS than the CASSCF structures, with the HF values being between those of CASSCF and QCISD. It is well known that HF tends to predict overly weak intramolecular hydrogen bonds.[34, 84, 86, 87] The fact that the CASSCF enol and keto structures were farther away from the TS for the proton transfer than

TABLE I.

Most Relevant Geometrical Parameters (in Ångstroms and Degrees) of Enol, Keto, and Transition-state Structures Optimized for Ground State at HF, B3LYP, QCISD, and CASSCF Levels of Theory.

	Enol				TS				Keto			
	HF[a]	B3LYP[b]	QCISD	CASSCF	HF[a]	B3LYP[b]	QCISD	CASSCF	HF[a]	B3LYP[b]	QCISD	CASSCF
$r(N_1—C_2)$	1.271	1.306 (1.304)	1.302	1.305	1.296	1.317 (1.317)	1.320	1.304	1.342	1.349 (1.349)	1.357	1.359
$r(C_2—C_3)$	1.461	1.445 (1.444)	1.461	1.469	1.419	1.425 (1.425)	1.426	1.421	1.359	1.382 (1.381)	1.377	1.361
$r(C_3—C_4)$	1.344	1.374 (1.373)	1.365	1.352	1.385	1.393 (1.393)	1.396	1.387	1.451	1.443 (1.442)	1.454	1.463
$r(C_4—O_5)$	1.318	1.324 (1.325)	1.342	1.334	1.269	1.299 (1.299)	1.300	1.299	1.210	1.246 (1.245)	1.245	1.240
$r(N_1—H_6)$	1.884	1.605 (1.627)	1.758	1.963	1.261	1.318 (1.318)	1.261	1.262	0.997	1.023 (1.022)	1.013	0.994
$r(O_5—H_6)$	0.961	1.027 (1.023)	0.991	0.950	1.186	1.164 (1.166)	1.199	1.185	2.089	1.899 (1.928)	1.990	2.173
$r(N_1—O_5)$	2.701	2.539 (2.553)	2.637	2.766	2.370	2.409 (2.410)	2.388	2.375	2.778	2.687 (2.703)	2.731	2.842
$\theta(N_1—H_6—O_5)$	141.2	148.8 (148.0)	145.7	140.4	151.1	152.0 (151.9)	152.2	152.1	124.5	131.4 (130.2)	127.9	123.2

[a] Values taken from ref. 26.

[b] Values in parentheses obtained using the D95++** basis set.

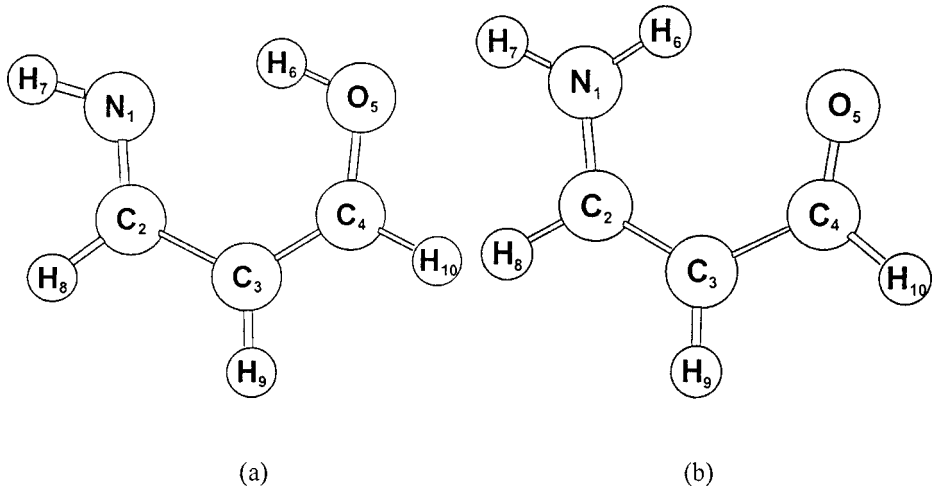

FIGURE 1. The ground-state geometries of: (a) the enol and (b) the keto tautomers of 1-amino-3-propenal optimized at the HF level.

the corresponding HF structures seems to indicate that the QCISD method is more reliable than the CASSCF method for describing the hydrogen bond. This may be related to the role of the dispersion interaction in this bond, which is less accurately described by CASSCF with a small active space than by QCISD. On the other hand, the enol and keto geometries yielded by B3LYP were closer to the TS of the proton transfer than the QCISD geometries, indicating that the hydrogen bond interaction may be overestimated by this method, which is in line with previous results.[25, 88, 89]

Adding diffuse functions to the D95** basis set at the B3LYP level does not introduce significant differences in the single and double-bond distances. However, the geometry parameters involved directly in the proton transfer are somewhat improved with respect to the QCISD reference values. In particular, the enol and keto geometries are separated farther from the TS of the proton transfer[25] and become closer to the QCISD geometries.

The change of the geometrical parameters after an electronic excitation depends on the rearrangement of the electron density resulting from the electron transition. The $^3n\pi^*$ excited state is obtained by exciting an electron from the HOMO-2 orbital, which essentially is the nitrogen lone-pair orbital in the enol form and the oxygen lone-pair orbital in the keto form, to the LUMO orbital, which has π^* character. The $^3\pi\pi^*$ excited state results from a one-electron transition from the π HOMO orbital to the LUMO orbital.[90] In the geometry optimizations of 1-amino-3-propenal in the two excited states, the molecule was kept planar. In fact, the planar structure is the most stable in the ground state and the two excited states according to the B3LYP, QCISD, and CASSCF calculations. In the case of the CIS method, some deviations from planarity in the excited states were found, especially for the enol form, as discussed previously.[26] As indicated by Scheiner et al.,[15, 33] inclusion of the electron correlation tends to favor the planar geometry in the excited states.

The changes in the N_1—H_6, H_6—O_5, and N_1—O_5 bond distances resulting from the electron excitations were similar for all the methods used (Table II). In the enol form, the N_1—H_6 and N_1—O_5 bond distances increased considerably and the H_6—O_5 bond length decreased upon excitations to the $^3\pi\pi^*$ and $^3n\pi^*$ states. Likewise, in the keto form, the H_6—O_5 and the N_1—O_5 bond distances increased, whereas the N_1—H_6 bond length decreased. As was the case for the ground state, these parameters were most affected by the inclusion of the electron correlation in the calculations. Although the changes in the geometries caused by electronic excitations were similar for all methods used, some noticeable differences among them appeared. As indicated for the ground state, DFT overestimated the hydrogen bond interaction in the $^3\pi\pi^*$ and $^3n\pi^*$ excited states, with the DFT geometries being closer to the proton-transfer TS geometries than the QCISD geometries. Also, for the excited states, CASSCF yielded geometries that were farther away from the TS structures than the QCISD geometries. CIS predicted a weaker intramolecular hydrogen bond than CASSCF, except for the keto form in the $^3\pi\pi^*$ excited state.

TABLE II.

Most Relevant Geometrical Parameters Involved in Proton Transfer (in Ångstroms and Degrees) of Enol, Keto, and Transition State Structures Optimized for $^3\pi\pi^*$ and $^3n\pi^*$ at CIS, B3LYP, QCISD, and CASSCF Levels of Theory.

	Enol				TS				Keto			
	CIS	B3LYP[a]	QCISD	CASSCF	CIS	B3LYP[a]	QCISD	CASSCF	CIS	B3LYP[a]	QCISD	CASSCF
$^3\pi\pi^*$												
$r(N_1—H_6)$	2.051	1.736 (1.753)	1.861	2.000	1.241	1.289 (1.292)	1.242	1.130	0.992	1.023 (1.023)	1.006	0.992
$r(O_5—H_6)$	0.949	1.006 (1.004)	0.983	0.953	1.231	1.217 (1.217)	1.254	1.400	2.222	1.947 (1.976)	2.226	2.224
$r(N_1—O_5)$	2.832	2.644 (2.655)	2.728	2.812	2.403	2.445 (2.446)	2.434	2.457	2.897	2.761 (2.776)	2.889	2.910
θ $(N_1—H_6—O_5)$	138.5	148.0 (147.4)	145.5	141.9	152.9	154.6 (154.4)	154.5	150.9	124.1	134.3 (133.0)	122.1	125.1
$^3n\pi^*$												
$r(N_1—H_6)$	2.377	2.061 (2.087)	2.149	2.288	1.216	1.406 (1.399)	1.326	1.250	0.991	1.010 (1.010)	1.006	0.991
$r(O_5—H_6)$	0.942	0.974 (0.974)	0.967	0.943	1.132	1.069 (1.076)	1.097	1.112	2.371	2.221 (2.238)	2.224	2.309
$r(N_1—O_5)$	3.098	2.883 (2.900)	2.952	3.027	2.240	2.393 (2.390)	2.345	2.282	2.972	2.895 (2.905)	2.887	2.933
$\theta(N_1—H_6—O_5)$	133.1	140.8 (139.8)	139.6	134.8	145.2	150.0 (149.7)	150.8	150.0	118.3	122.8 (122.2)	122.1	120.1

[a] Values in parentheses obtained using the D95++** basis set.

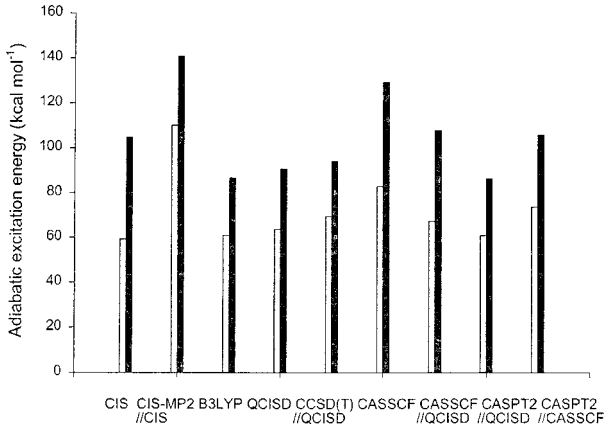

FIGURE 2. Adiabatic excitation energies corresponding to excitations from the ground state to the $^3\pi\pi^*$ (shaded bars) and $^3n\pi^*$ (filled bars) excited states for the enol form computed using the CIS, CIS-MP2//CIS, B3LYP, QCISD, CCSD(T)//QCISD, CASSCF, CASSCF//QCISD, CASPT2//QCISD, and CASPT2//CASSCF methods.

ENERGETIC PARAMETERS

Figure 2 shows a graphical comparison of the adiabatic excitation energies for the enol form computed with the different methodologies. Given the lack of experimental results for the system studied, and because it has been shown that CCSD(T) yields excitation energies typically within 5 kcal mol^{-1} of experiment,[91, 92] the CCSD(T)//QCISD results, as mentioned earlier, are used here as the reference values for evaluating the performance of the other methods. All methods predicted the same energetic order for the two excited states considered; that is, the $^3\pi\pi^*$ excited state was lower in energy than the $^3n\pi^*$ excited state. B3LYP and QCISD predicted adiabatic excitation energies quite close to the CCSD(T)//QCISD values. On the other hand, the adiabatic excitation energies obtained with CASSCF were largely overestimated compared with the reference values. It is of interest to note that a noticeable improvement was obtained when the QCISD geometries were employed. The $^3n\pi^*$ adiabatic excitation energy predicted by CIS was also overestimated,[92, 93] although the difference with respect to the reference value was smaller than that yielded by the CASSCF method. Introduction of dynamical correlation through the MP2 method to the CIS energies has been shown to result in a large increase in the adiabatic excitation energies.[93] As a result, the CIS-MP2 energies differed most from the reference values. By contrast, the effect of dynamical correlation introduced by the second-order correction to the CASSCF method brought them closer to the reference values, irrespective of the method used for the geometry optimization. As pointed out by Scheiner et al.[24] there is no fundamental reason why the addition of correlation energy should necessarily raise or lower the excitation energy. Although, in principle, one could expect a smaller effect of the dynamic electron correlation in the excited states than in the ground state, because the electrons in the excited states are separated more due to single occupancies of some of the orbitals in these states, it is also true that, for these states, the nondynamic correlation effects and the core correlation effects may be larger. The closest CASPT2 adiabatic excitation energies to the CCSD(T)//QCISD results were obtained using the QCISD geometries.

Figures 3 and 4 illustrate the difference between the relative energy of the two tautomers and the energy barrier for the proton transfer from the enol form, respectively, yielded by each method and that obtained at the CCSD(T)//QCISD level for each of the states. Let us first comment on the energetic parameters in the ground state. All methods predicted the keto tautomer to be the most stable form. The B3LYP and MP2//HF methods underestimated the energy barrier for the proton transfer. By contrast, HF and CASSCF yielded energy barriers considerably higher than CCSD(T)//QCISD. The CASSCF energy barrier was reduced only slightly when geometries other than CASSCF were used and, surprisingly, it was larger than the HF barrier (except for the case when DFT geometries were used). However, introducing the dynamic energy correlation to the CASSCF wave function through CASPT2 resulted in an energy barrier closer to the reference value. This is a clear indication of the importance of accounting for the dynamic electron correlation effects in describing the proton transfer process.[20, 79, 80]

Concerning the energy difference of the two tautomers in the excited states, both tautomers had, according to the CCSD(T)//QCISD results, nearly the same energy in the $^3\pi\pi^*$ state whereas the keto form was about 20 kcal mol^{-1} more stable than the enol form in the $^3n\pi^*$ state. CASPT2 reproduced these results quite well, irrespective of the method used to optimize the geometries. As found for the ground state, HF and CASSCF yielded the worst values, especially for the $^3n\pi^*$ excited state.

The CCSD(T)//QCISD energy barriers in the $^3\pi\pi^*$ and $^3n\pi^*$ states were about 4 and 2 kcal mol^{-1} larger, respectively, than in the ground state. Inter-

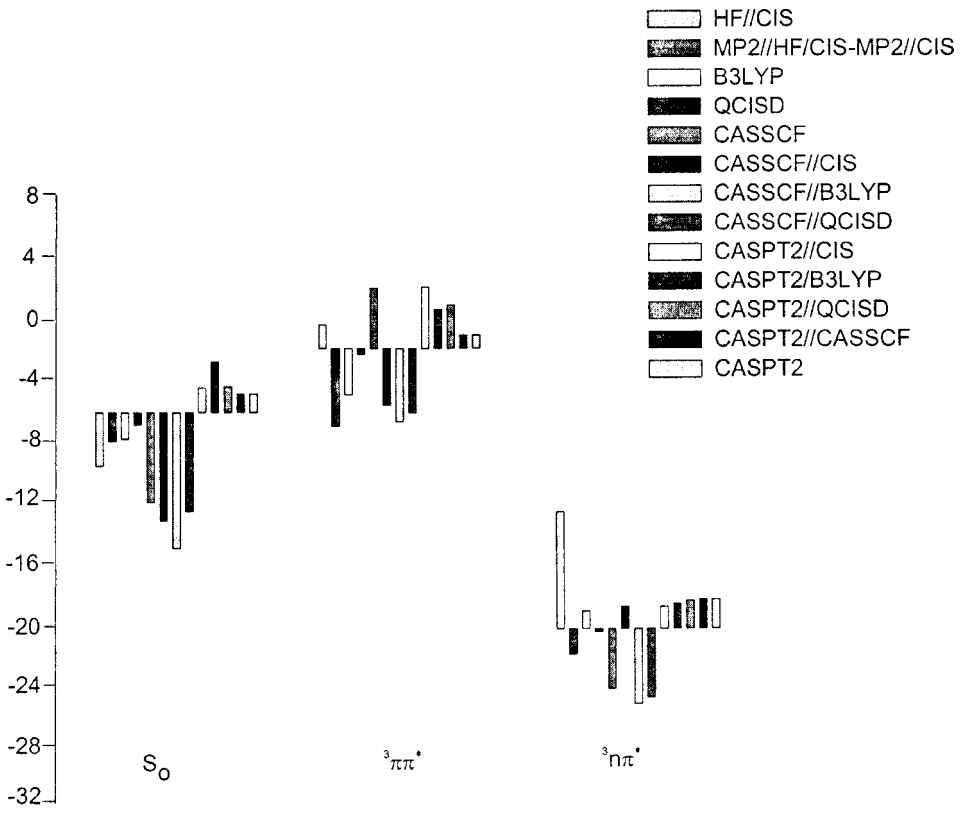

FIGURE 3. Difference between the relative energy of the two tautomers provided by each method and that obtained at the CCSD(T)//QCISD level for the ground state and for the $^3\pi\pi^*$ and $^3n\pi^*$ excited states. The CCSD(T)//QCISD relative energies are −5.2, −1.7, and −21.0, respectively.

estingly, for all methods, the errors in the computed barrier heights were larger in the excited states than in the ground state. The QCISD method consistently gave energy barriers that were somewhat larger than the CCSD(T)//QCISD barriers. On the other hand, B3LYP predicted barriers that were too low. Remarkably, the B3LYP energy barriers increased slightly when the diffuse functions were included in the basis set,[25] as expected from the geometrical changes described in the previous section.[15, 16] CIS and CASSCF yielded much higher energy barriers in comparison to the CCSD(T)//QCISD barriers.[33, 80] The MP2 corrections to CIS and CASSCF drastically reduced the energy barriers. The CIS-MP2//CIS energy barriers approached the reference values, although they were somewhat underestimated.[15, 16, 18, 24, 26, 33, 39] On the other hand, the CASPT2 method yielded very similar energy barriers to the reference values. Thus, we conclude that the CIS and CASSCF ESIPT energy barriers were not reliable and the dynamical electronic correlation effects must be accounted for if quantitatively correct results are needed.[79, 80]

It is worth noting that the excited-state CASPT2 energy barriers most different from the CCSD(T)//QCISD results were those obtained with the CASSCF geometries. This indicates that the CASSCF method with a medium-sized active space poorly predicts the TS geometries, and that dynamic electron correlation effects have to be accounted for to obtain more accurate structural parameters. To further investigate this point we attempted to locate the TS with the CASPT2 method. Because CASPT2 analytical gradients had not yet been implemented, and a complete geometry optimization would be too time-consuming at this level of theory, we used an approximate approach by following the CASPT2 potential energy surface along the proton-transfer reaction coordinate. This coordinate was chosen to be the N_1—H_6 bond distance. We calculated the CASPT2 energy at nine N_1—H_6 bond distances with the rest of the geometry parameters optimized for each point at the CASSCF level.

Table III summarizes the CASSCF-optimized geometry corresponding to the maximum CASPT2 energy point along the reaction coordinate in each

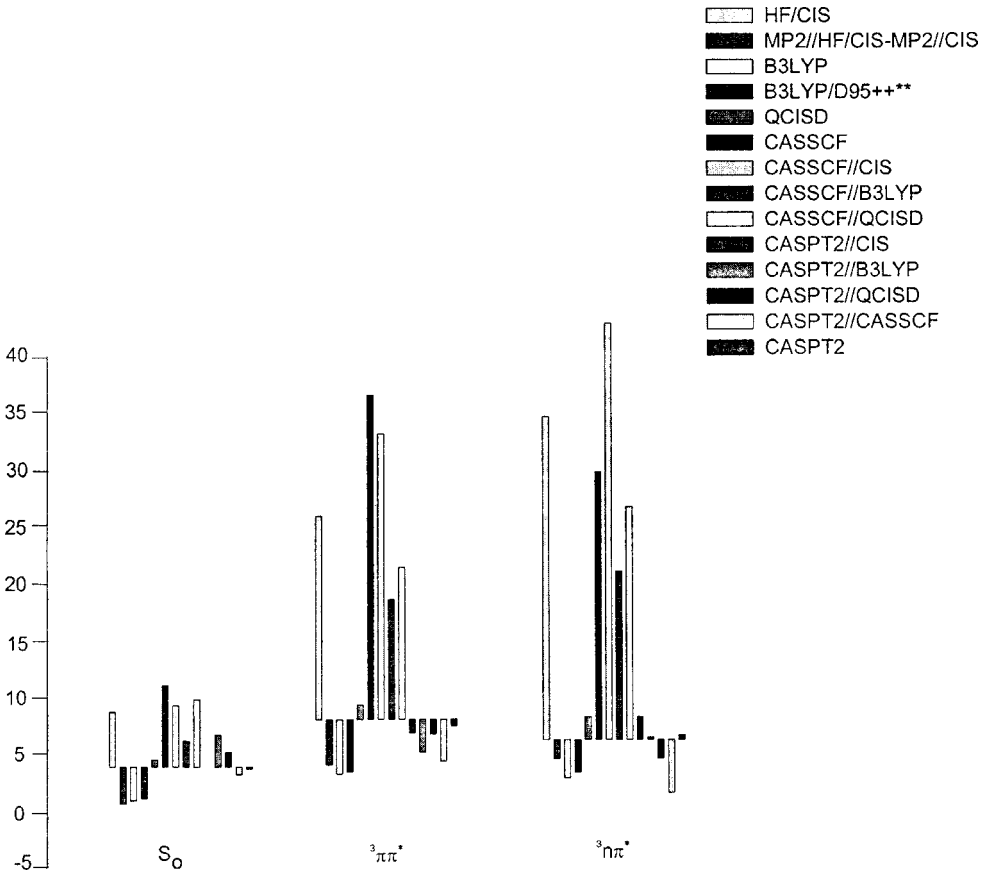

FIGURE 4. Difference between the energy barrier provided by each method and that obtained at the CCSD(T)//QCISD level for the ground state and for the $^3\pi\pi^*$ and $^3n\pi^*$ excited states. The CCSD(T)//QCISD energy barriers are 3.9, 8.2, and 5.8, respectively.

TABLE III.
Most Relevant Geometrical Parameters (in Ångstroms and Degrees) of Approximated TS for CASPT2 Method and Relative Energy of Two Tautomers and Energy Barrier for Proton Transfer of Enol Form (kcal mol^{-1}) Obtained Following the Potential Energy Surface along the Reaction Coordinate.

	S_0	$^3\pi\pi^*$	$^3n\pi^*$
$r(N_1—C_2)$	1.305	1.379	1.386
$r(C_2—C_3)$	1.419	1.378	1.401
$r(C_3—C_4)$	1.388	1.461	1.384
$r(C_4—O_5)$	1.273	1.346	1.356
$r(N_1—H_6)$	1.250	1.250	1.300
$r(O_5—H_6)$	1.239	1.125	1.010
$r(N_1—O_5)$	2.407	2.337	2.268
$\theta(N_1—H_6—O_5)$	150.6	158.1	157.3
$\Delta E_{k\text{-}e}$	−4.0	−0.8	−19.0
$\Delta E^{\ddagger}_{TS\text{-}e}$	3.7	7.6	6.2

state. The structure for this point in the ground state was not much different from that of the CASSCF TS (Table I). However, the CASPT2 TS structure for the excited states was closer to the enol form than the corresponding CASSCF TSs. Moreover, the geometry of the approximate CASPT2 TS for each excited state was closer to the QCISD TS than to the CASSCF TS. The importance of the correlation effects can also be illustrated by comparing the CASSCF and CASPT2 energy profiles (Fig. 5). The CASPT2 maximum energy points in both excited states were displaced to larger $N_1—H_6$ values than the corresponding CASSCF TSs. The calculated CASPT2 energy barriers in the ground state and in the two excited states are also given in Table III. The value for the ground state is nearly equal to that obtained with the CASSCF TS. For the excited states, the values were considerably larger and very close to the CCSD(T)//QCISD values. Clearly, following the reaction coordinate leads to an improvement of results. On the other hand, the relative

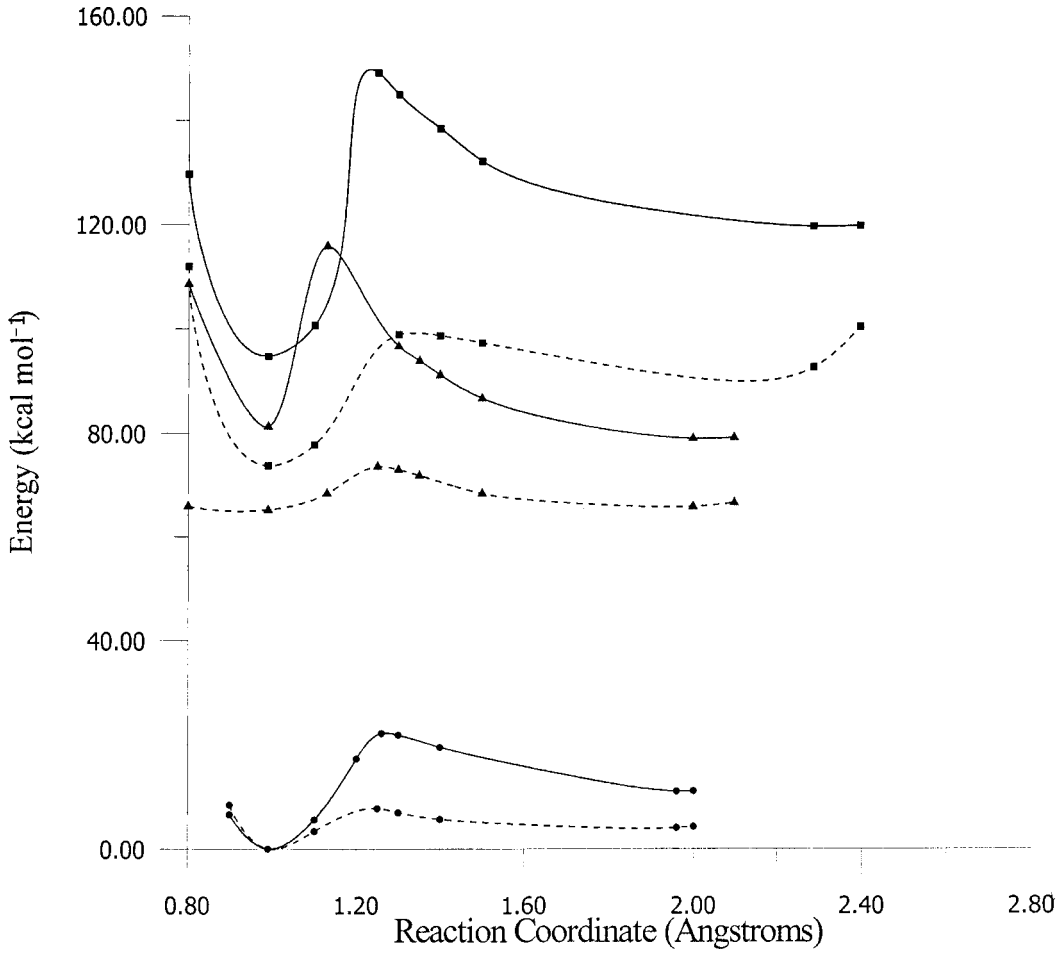

FIGURE 5. Relative CASSCF (solid line) and CASPT2 (dashed line) energy profiles, both referred to the corresponding keto form in the ground state, for the ground state (•) and for the $^3\pi\pi^*$ (▲) and $^3n\pi^*$ (■) excited states.

energies of the two tautomers was the same in CASPT2//CASSCF and CASPT2 calculations, indicating that the dynamic energy correlation was not as important at the energy minimum points as it was in the TS region.

Conclusions

A detailed analysis of the geometries and energies computed at different theoretical levels has been performed for the proton-transfer process in the ground state and in the $^3\pi\pi^*$ and $^3n\pi^*$ excited states of 1-amino-3-propenal.

It was shown that CASSCF with a medium-sized active space describes structures of the enol and keto forms of this system that are noticeably more distant from the proton-transfer TS than those predicted by QCISD. In particular, for the ground state, the CASSCF enol and keto forms were even more distant from QCISD TS than the tautomeric HF structures. On the other hand, B3LYP predicted enol and keto structures that were too close to the proton transfer QCISD TS.

Concerning the adiabatic excitation energies, the B3LYP and QCISD methods were shown to reproduce the CCSD(T)//QCISD results quite well. Larger differences were found in the CASSCF results, which were considerably overestimated. Introduction of the dynamic correlation energy to the CASSCF results using CASPT2 yielded values close to the CCSD(T)//QCISD results, especially if the QCISD geometries were used in the calculations. CIS-MP2 predicted the worst adiabatic excitation energies.

Both CIS and CASSCF provided inaccurate descriptions of the PT processes by yielding energy barriers that were too large, a poor description of the hydrogen bond, and inaccurate TS geometries, especially in the excited states. This indicates that

the correlation effects neglected in these methods were essential for a correct quantitative description of ESIPT processes. The second-order perturbation approach applied in conjunction with the CIS and CASSCF methods diminished the energy barriers. CIS-MP2 yielded energy barriers that were somewhat underestimated, whereas CASPT2 gave energy parameters that were in good agreement with the CCSD(T)//QCISD results. The energy barriers computed by the B3LYP method were systematically too low, although the error was comparable for the different electronic states.

In summary, in the description of ESIPT processes, the CIS-MP2//CIS method provides a good compromise between the accuracy and the computational cost involved in the calculations, yielding results that are qualitatively correct, but cannot be relied upon in quantitative predictions. In our analysis we have not found a low-cost method among the methods studied that is capable of quantitatively describing the ESIPT process. The least time-consuming approach that we can recommend to produce quantitative results is to carry out CASPT2 calculations with a medium-sized active space using CIS-optimized geometries.

Note Added in Proof. After completion of this work, a study[94] on the use of different methodologies to analyze ESIPT processes in a series of molecules related to malonaldehyde has appeared. The study by Kar, Scheiner, and Cuma carries out single-point energy calculations at different levels of theory using the CIS-optimized geometries. Despite the fact that the authors do not explore the effect of geometry optimization at higher levels of theory, their conclusions are very similar to those presented here.

Acknowledgments

The authors acknowledge the Centre de Supercomputació de Catalunya (CESCA) for the generous allocation of computing time.

Supplementary Material

The supplementary material contains tables with the cartesian coordinates of the optimized enol, keto, and transition-state structures; the adiabatic excitation energies; the relative energy of the two tautomers; and the energy barriers for all different methods used and for the three states analyzed.

References

1. (a) Chou, P.; McMorrow, D.; Aartsma, T. J.; Kasha, M. J Phys Chem 1984, 88, 4596; (b) Parthenopoulos, D. A.; McMorrow, D.; Kasha, M. J Phys Chem 1991, 95, 2668; (c) Macinnis, J. M.; Kasha, M. Chem Phys Lett 1988, 151, 375.
2. Parthenopoulos, D. A.; Kasha, M. Chem Phys Lett 1988, 146, 77.
3. (a) Ernsting, N. P.; Nikolaus, B. Appl Phys B 1986, 39, 155; (b) Liphardt, M.; Goonesekera, A.; Jones, B. E.; Ducharme, S.; Takacs, J. M.; Zhang, L. Science 1994, 263, 367; (c) Douhal, A.; Sastre, R. Chem Phys Lett 1994, 219, 91.
4. Martinez, M. L.; Cooper, W. C.; Chou, P.-T. Chem Phys Lett 1992, 193, 151.
5. Otterstedt, J.-E. A. J Chem Phys 1973, 58, 5716.
6. Ormson, S. M.; Brown, R. G. Prog React Kinet 1994, 19, 45.
7. Werner, T. J Phys Chem 1979, 83, 320.
8. Löwdin, P.-O. Rev Mod Phys 1963, 35, 724.
9. Pullman, B.; Pullman, A. Adv Heterocycl Chem 1971, 13, 77.
10. Douhal, A.; Lahmani, F.; Zewail, A. H. Chem Phys 1996, 207, 477.
11. Duan, X.; Scheiner, S. Chem Phys Lett 1993, 204, 36.
12. Sobolewski, A. L.; Domcke, W. Chem Phys Lett 1993, 211, 82.
13. Sobolewski, A. L. Chem Phys Lett 1993, 211, 293.
14. Sobolewski, A. L.; Domcke, W. Chem Phys 1994, 184, 115.
15. Luth, K.; Scheiner, S. J Phys Chem 1994, 98, 3582.
16. Luth, K.; Scheiner, S. J Phys Chem 1995, 99, 7352.
17. Estévez, C. M.; Bach, R. D.; Hass, K. C.; Schneider, W. F. J Am Chem Soc 1997, 119, 5445.
18. Guallar, V.; Moreno, M.; Lluch, J. M.; Amat-Guerri, F.; Douhal, A. J Phys Chem 1996, 100, 19789.
19. Sobolewski, A. L.; Adamowicz, L. Chem Phys 1996, 213, 181.
20. Sobolewski, A. L.; Adamowicz, L. Chem Phys 1995, 193, 67.
21. Sobolewski, A. L.; Adamowicz, L. Chem Phys Lett 1995, 234, 94.
22. Sobolewski, A. L.; Adamowicz, L. J Phys Chem 1995, 99, 14277.
23. Sobolewski, A. L.; Adamowicz, L. J Chem Phys 1995, 102, 5708.
24. Scheiner, S.; Kar, T.; Cuma, M. J Phys Chem A 1997, 101, 5901.
25. Barone, V.; Adamo, C. J Chem Phys 1996, 105, 11007.
26. Forés, M.; Duran, M.; Solà, M. Chem Phys 1998, 234, 1.
27. Hass, K. C.; Schneider, W. F.; Estévez, C. M.; Bach, R. D. Chem Phys Lett 1996, 263, 414.
28. Forés, M.; Duran, M.; Solà, M.; Adamowicz, L. J Phys Chem A 1999, 103, 4413.
29. Kieninger, M.; Suhai, S. Int J Quantum Chem 1994, 52, 465.
30. Van Duijneveldt-van de Rijdt, J. G. C. M.; Van Duijneveldt, F. B. J. Chem Phys 1992, 97, 5019.
31. Laforgue, A.; Brucena-Grimbert, C.; Laforghe-Kantzer, D.; Del Re, G.; Barone, V. J Phys Chem 1986, 86, 4436.
32. Scheiner, S. Acc Chem Res 1985, 18, 174.
33. Rovira, M. C.; Scheiner, S. J Phys Chem 1995, 99, 9854.
34. Scheiner, S. In: Truhlar, D. G., ed. Hydrogen Bonding. A Theoretical Perspective; Oxford University Press: New York, 1997.

35. Del Bene, J. G.; Ditchfield, R.; Pople, J. A. J Chem Phys 1971, 55, 2236.
36. Foresman, J. B.; Head-Gordon, M.; Pople, J. A.; Frisch, M. J. J Phys Chem 1992, 96, 135.
37. Grimme, S. Chem Phys Lett 1996, 259, 128.
38. Stanton, J. F.; Gauss, J.; Ishikawa, N.; Head-Gordon, M. J Chem Phys 1995, 103, 4160.
39. Barone, V.; Adamo, C. Int J Quantum Chem 1997, 61, 429.
40. Schlegel, H. B. J Chem Phys 1986, 84, 4530.
41. Cizek, J. J Chem Phys 1966, 45, 4256.
42. Taylor, P. R.; Bacskay, G. B.; Hush, N. S.; Hurley, A. C. Chem Phys Lett 1976, 41, 444.
43. Pople, J. A.; Krishnan, R.; Schlegel, H. B.; Binkley, J. S. Int J Quantum Chem 1978, 14, 545.
44. (a) Bartlett, R. J.; Purvis, G. D. Int J Quantum Chem 1978, 14, 561; (b) Bartlett, R. J. Ann Rev Phys Chem 1981, 32, 359.
45. Purvis, G. D.; Bartlett, R. J. J Chem Phys 1982, 76, 1910.
46. Urban, M.; Noga, J.; Cole, S. J.; Bartlett, R. J. J Chem Phys 1985, 83, 4041.
47. Raghavachari, K. J Chem Phys 1985, 82, 4607.
48. Pople, J. A.; Head-Gordon, M.; Raghavachari, K. J Chem Phys 1987, 87, 5968.
49. Wolinski, K.; Pulay, P. J Chem Phys 1989, 90, 3647.
50. Chen, W.; Schlegel, H. B. J Chem Phys 1994, 101, 5957.
51. Sekino, H.; Barlett, R. J. J Chem Phys 1985, 82, 4225.
52. Roos, B. O. In: Lawley, K. P., ed. Advances in Chemical Physics. Ab initio Methods in Quantum Chemistry. Part 2; Wiley: New York, 1987 399.
53. Andersson, K.; Malmqvist, P.-Å.; Roos, B. O.; Sadlej, A. J.; Wolinski, K. J Phys Chem 1990, 94, 5483.
54. Andersson, K.; Malmqvist, P.-Å.; Roos, B. O. J Chem Phys 1992, 96, 1218.
55. Andersson, K.; Roos, B. O. In: Yarkony, R., ed. Modern Electron Structure Theory; Vol. 1; World Scientific: New York, 1994.
56. Parr, R. G.; Yang, W. Density Functional Theory of Atoms and Molecules; Oxford University Press: Oxford, UK, 1989.
57. Johnson, B. G.; Gill, P. M. W.; Pople, J. A. J Chem Phys 1993, 98, 5612.
58. Seminario, J. M.; Politzer, P. Modern Density Functional Theory: A Tool for Chemistry; Elsevier: New York, 1995.
59. Ziegler, T. Chem Rev 1991, 91, 651.
60. Cramer, C. J.; Dulles, F. J.; Giesen, D. J.; Almlöf, J. Chem Phys Lett 1995, 245, 165.
61. Kasha, M.; Heldt, J.; Gormin, D. J Phys Chem 1995, 99, 7281.
62. Wood, P. D.; Redmond, R. W. J Am Chem Soc 1996, 118, 4256.
63. (a) Al-Ansari, I. A. Z. J Lumin 1997, 71, 83; (b) Das, S. K.; Bansal, A.; Dogra, S. K. Bull Chem Soc Jpn 1997, 70, 307; (c) Mosquera, M.; Penedo, J. C.; Ríos-Rodríguez, M. C.; Rodríguez-Prieto, F. J Phys Chem 1996, 100, 5398.
64. Roberts, E. L.; Dey, J.; Warner, I. M. J Phys Chem 1996, 100, 19681.
65. Yang, G.; Morlet-Savary, F.; Peng, Z.; Wu, S.; Fouassier, J. P. Chem Phys Lett 1996, 256, 536.
66. Becke, A. D. J Chem Phys 1993, 98, 5648.
67. Lee, C.; Yang, W.; Parr, R. G. Phys Rev B 1988, 37, 785.
68. Catalán, J.; Palomar, J.; de Paz, J. L. G. J Phys Chem A 1997, 101, 7914.
69. Novoa, J. J.; Sosa, C. J Phys Chem 1995, 99, 15837.
70. Pudzianowski, A. T. J Phys Chem 1996, 100, 4781.
71. del Bene, J. E.; Person, W. B.; Szczepaniak, K. J Phys Chem 1995, 99, 10705.
72. In the case of the CASSCF TS geometry, the frequency calculations were calculated numerically using the STO-3G basis set.
73. Raghavachari, K.; Trucks, G. W.; Pople, J. A.; Head-Gordon, M. Chem Phys Lett 1989, 157, 479.
74. Bartlett, R. J.; Watts, J. D.; Kucharski, S. A.; Noga, J. Chem Phys Lett 1990, 165, 513.
75. Wang, J.; Becke, A. D.; Smith, V. H., Jr. J Chem Phys 1995, 102, 3477.
76. Baker, J.; Scheiner, A.; Andzelm, J. Chem Phys Lett 1993, 216, 380.
77. Wang, J.; Eriksson, L. A.; Boyd, R. J.; Shi, Z.; Johnson, B. G. J Phys Chem 1994, 98, 1844.
78. Adamo, C.; Barone, V.; Fortunelli, A. J Phys Chem 1994, 98, 8648.
79. Forés, M.; Adamowicz, L. J Comput Chem 1999, 20, 1422.
80. Sobolewski, A. L.; Domcke, W. J Phys Chem A 1999, 103, 4494.
81. Dunning, T. H., Jr.; Hay, P. J. In: Schaefer, H. F., III, ed. Methods of Electronic Structure Theory; Plenum: New York, 1977.
82. Clark, T.; Chandrasekhar, J.; Spitznagel, G. W.; Schleyer, P. V. R. J Comput Chem 1983, 4, 294.
83. Andersson, K.; Fülscher, M. P.; Karlström, G.; Lindh, R.; Malmqvist, P.-Å.; Olsen, J.; Roos, B. O.; Sadlej, A. J.; Blomberg, M. R. A.; Siegbahn, P. E. M.; Kellö, V.; Noga, J.; Urban, M.; Widmark, P.-O. MOLCAS, Version 3, Lund University, Sweden, 1994.
84. Andersson, K.; Blomberg, M. R. A.; Fülscher, M. P.; Karlström, G.; Lindh, R.; Malmqvist, P.-Å.; Neogrády, P.; Olsen, J.; Roos, B. O.; Sadlej, A. J.; Sadlej, M.; Schütz, M.; Seijo, L.; Serrano-Andrés, L.; Siegbahn, P. E. M.; Widmark, P.-O. MOLCAS, Version 4, Lund University, Sweden, 1997.
85. Frisch, M. J.; Trucks, G. W.; Schlegel, H. B.; Gill, P. M. W.; Johnson, B. G.; Robb, M. A.; Cheeseman, J. R.; Keith, T. A.; Petersson, G. A.; Montgomery, J. A.; Raghavachari, K.; Al-Laham, M. A.; Zakrzewski, V. G.; Ortiz, J. V.; Foresman, J. B.; Cioslowski, J.; Stefanov, B.; Nanayakkara, A.; Challacombe, M.; Peng, C. Y.; Ayala, P. Y.; Chen, W.; Wong, M. W.; Andrés, J. L.; Replogle, E. S.; Gomperts, R.; Martin, R. L.; Fox, D. J.; Binkley, J. S.; Defrees, D. J.; Baker, J.; Stewart, J. J. P.; Head-Gordon, M.; Gonzalez, C.; Pople, J. A. GAUSSIAN 94, Revision B.2; Gaussian, Inc., Pittsburgh, PA, 1995.
86. Duan, X.; Scheiner, S. Chem Phys Lett 1993, 204, 36.
87. Sim, F.; St-Amant, A.; Papai, I.; Salahub, D. R. J Am Chem Soc 1992, 114, 4391.
88. Jursic, B. S. J Mol Struct (Theochem) 1997, 417, 89.
89. Zhang, Q.; Bell, R.; Truong, T. N. J Phys Chem 1995, 99, 592.
90. See ref. 26 for a depiction of the HF orbitals involved in the $n\pi^*$ and $\pi\pi^*$ transitions.
91. Baltan, E. E.; Schaefer, H. F., III J Am Chem Soc 1993, 115, 6207.
92. Love, D. E.; Nachligallova, D.; Jordan, K. D.; Lawson, J. M.; Paddon-Row, M. N. J Am Chem Soc 1996, 118, 1235.
93. Hadad, C. M.; Foresman, J. B.; Wiberg, K. B. J Phys Chem 1993, 97, 4293.
94. Kar, T.; Scheiner, S.; Cuma, M. J Chem Phys 1999, 111, 849.